ISSN 1063-7710, Acoustical Physics, 2016, Vol. 62, No. 2, pp. 179–186. © Pleiades Publishing, Ltd., 2016.
Original Russian Text © D.A. Gubaidullin, Yu.V. Fedorov, 2016, published in Akusticheskii Zhurnal, 2016, Vol. 62, No. 2, pp. 178–186.

PHYSICAL ACOUSTICS

Sound Waves in a Liquid with Polydisperse Vapor–Gas Bubbles

D. A. Gubaidullin and Yu. V. Fedorov

Institute of Mechanics and Engineering, Kazan Science Center, Russian Academy of Sciences, ul. Lobachevskogo 2/31, Kazan, 420111 Russia

e-mail: gubaidullin@imm.knc.ru; kopperfildd@yandex.ru

Received May 26, 2015

Abstract—A mathematical model is presented for the propagation of plane, spherical, and cylindrical sound waves in a liquid containing polydisperse vapor–gas bubbles with allowance for phase transitions. A system of integro-differential equations is constructed to describe perturbed motion of a two-phase mixture, and a dispersion relation is derived. An expression for equilibrium sound velocity is obtained for a gas–liquid or vapor–liquid mixture. The theoretical results agree well with the known experimental data. The dispersion curves obtained for the phase velocity and the attenuation coefficient in a mixture of water with vapor–gas bubbles are compared for various values of vapor concentration in the bubbles and various bubble distributions in size. The evolution of pressure pulses of plane and cylindrical waves is demonstrated for different values of the initial vapor concentration in bubbles. The calculated frequency dependence of the phase sound velocity in a mixture of water with vapor bubbles is compared with experimental data.

Keywords: sound waves, bubbly liquid, vapor–gas bubbles, phase transitions, dispersion relation

DOI: 10.1134/S1063771016020068

INTRODUCTION

It is well known that the presence of vapor or gas bubbles in a liquid considerably affects its acoustic properties. Numerous publications have been devoted to theoretical studies of harmonic disturbances in such mixtures. The fundamental approaches used in studying the acoustics of bubbly liquids were described in [1, 2]. The basic features of a two-phase medium with a bubbly structure were considered in [3]. Publications concerning wave propagation in liquids containing constant-mass bubbles and publications devoted to wave dynamics with vapor bubbles or soluble gas bubbles were reviewed. In [4], the problems and properties of two-phase flows with solid particles, droplets, and bubbles were described. The basic characteristics of two-phase flows were presented along with their simulation methods. The results of theoretical calculations and experimental studies of two-phase flows were considered. The propagation of small disturbances in a liquid with gas bubbles was theoretically [5–9] and experimentally [10–12] investigated. In [13, 14], the theoretical dependences of the phase velocity and the attenuation coefficient on the frequency of disturbances were found to agree well with experimental data [10, 11]. In [15–17], the propagation of small disturbances in a liquid with monodisperse vapor bubbles was theoretically investigated. A considerable effect of phase transitions on the positions of the dispersion curves was demonstrated.

In [18, 19], the results of experimental studies of low-frequency pressure wave propagation in a vapor–liquid flow moving through a densely packed layer of solid spherical particles were presented. The results of the experiments allowed determination of the characteristic parameters and conditions corresponding to the coincidence between the pressure wave propagation velocity and the thermodynamic equilibrium sound velocity in a vapor–liquid mixture. For the first time, it was experimentally demonstrated that the velocity of low-frequency disturbances in a vapor–water medium may be several meters per second, which is close to the Landau sound velocity [20].

In [21, 22], the propagation of small disturbances in a two-phase medium was considered for a medium whose gaseous phase was a two-component mixture of the vapor of the liquid phase and an inert gas not involved in the mass transfer between phases. A dispersion relation was derived. A strong effect of the vapor concentration on the positions of the dispersion curves was demonstrated.

Here, we generalize the model given in [22] to the case of polydisperse bubbles with a continuous distribution of inclusions in size. Recent publications [23–25] testify to the topicality of this subject.

BASIC EQUATIONS

We consider the propagation of plane, spherical, and cylindrical waves in a liquid with polydisperse vapor–gas bubbles under the following assumptions. The wavelength of sound is much greater than the mean distance between bubbles and far exceeds the size of the bubbles themselves. The volume content of bubbles is small: $\alpha_2 \ll 1$. Heat-and-mass transfer is only significant for the phase interaction processes. In addition, the mass transfer process involves only the vapor component; i.e., the vapor can condense or evaporate.

The disperse composition of the mixture is characterized by the distribution function $N(a)$, where a is the bubble radius, with the following property:

$$N(a) = 0 \text{ for } a < a_{\min} \text{ and } a > a_{\max}.$$

The number of vapor–gas bubbles δn falling within the radius interval from a to $a + da$ in a unit volume of the mixture is determined as

$$\delta n = N(a)da.$$

The total number of bubbles n in a unit volume and the volume contents of the disperse phase α_2 and the host phase α_1 are determined by the integrals

$$n = \int_{\Delta a} N(a)da,\ \alpha_2 = \frac{4\pi}{3}\int_{\Delta a} N(a)a^3 da,$$

$$\alpha_1 + \alpha_2 = 1,\ \Delta a = [a_{\min}, a_{\max}].$$

The main parameters of the mixture are as follows:

$$\rho_1 = \rho_1^\circ\alpha_1,\ \rho_2 = \rho_2^\circ\alpha_2 = \int_{\Delta a} N(a)g(a)da,\ g(a) = \frac{4\pi}{3}a^3\rho_2^\circ,$$

$$m = \frac{\rho_2}{\rho_1},\ k_V = \frac{\rho_V}{\rho_2},\ k_G = \frac{\rho_G}{\rho_2},\ k_V + k_G = 1.$$

Here, ρ°, ρ are the true and mean densities of the mixture, g is the mass of an individual inclusion, m is the mass content, and k_i is the mass concentration of the vapor ($i = V$) and gas ($i = G$) components of the disperse phase.

For small disturbances in a spatially homogeneous (initially unperturbed) monodisperse mixture, the linearized equations describing conservation of mass, conservation of the number of bubbles, conservation of momentum, and conservation of energy have the form [22]

$$\frac{\partial\rho_1'}{\partial t} + \rho_{10}\left(\frac{\partial v_1'}{\partial r} + \theta\frac{v_1'}{r}\right) = -n_0 j',$$

$$\frac{\partial\rho_V'}{\partial t} + \rho_{V0}\left(\frac{\partial v_1'}{\partial r} + \theta\frac{v_1'}{r}\right) = n_0 j',$$

$$\frac{\partial\rho_2'}{\partial t} + \rho_{20}\left(\frac{\partial v_1'}{\partial r} + \theta\frac{v_1'}{r}\right) = n_0 j',\ \frac{\partial n'}{\partial t} + n_0\left(\frac{\partial v_1'}{\partial r} + \theta\frac{v_1'}{r}\right) = 0,$$

$$\rho_{10}\frac{\partial v_1'}{\partial t} + \frac{\partial p_1'}{\partial x} = 0,\ \rho_{10}c_{p1}\frac{\partial T_1'}{\partial t} = n_0 q_{1\Sigma},$$

$$\rho_{20}c_{p2}\frac{\partial T_2'}{\partial t} = \alpha_{20}\frac{\partial p_2'}{\partial t} + n_0 q_{2\Sigma},\ n_0 q_{1\Sigma} + n_0 q_{2\Sigma} = -l_0 n_0 j'.$$

Here and below, subscripts 1 and 2 indicate parameters of the host and disperse phases, respectively; V and G correspond to the vapor and gas components of the disperse phase; and Σ corresponds to the interface. The primes indicate perturbations of parameters, subscript 0 corresponds to the initial unperturbed state, r is a coordinate, t is time, v_1 is velocity, p is pressure, w is the velocity of the radial motion of bubbles, c_p is the specific heat, l_0 is the specific heat of evaporation, T is temperature, and θ is a parameter determining the wave geometry.

The heat flows and intensity of phase transitions are determined by the expressions [21]

$$q_{1\Sigma} = g_0 c_{p1}\frac{T_\Sigma' - T_1'}{\tau_{T1}},\ q_{2\Sigma} = g_0 c_{p2}\frac{T_\Sigma' - T_2'}{\tau_{T2}},$$

$$j' = \frac{g_0}{1 - k_{V0}}\frac{k_{V\Sigma}' - k_V'}{\tau_m},$$

$$\tau_{T1} = \frac{2c_{p1}\rho_2^\circ a^2}{3\mathrm{Nu}_1\lambda_1},\ \tau_{T2} = \frac{2c_{p2}\rho_2^\circ a^2}{3\mathrm{Nu}_2\lambda_2},\ \tau_m = \frac{2a^2}{3\mathrm{Sh}_1 D_1},$$

$$c_{p2} = k_{V0}c_{pV} + k_{G0}c_{pG},\ \lambda_2 = k_{V0}\lambda_V + k_{G0}\lambda_G.$$

Here, Sh_1 is the dimensionless mass transfer coefficient or the Sherwood number, D_1 is the diffusion coefficient, λ is the thermal conductivity coefficient, and Nu is the Nusselt number.

The system of linear integro-differential equations describing the propagation of sound waves in a liquid with polydisperse vapor–gas bubbles can be obtained by integrating the linearized equations of mass conservation, conservation of momentum, and conservation of energy over the bubble radius a from $a_{\min}$ to $a_{\max}$. We derive the conservation of mass equation for vapor–gas bubbles under the assumption that variation in the disperse phase with radii from a to $a + da$ is described by the motion of the monodisperse mixture with the characteristic radius a. Then, $\delta\rho_2 = N(a)g_0(a)\delta a$ is the mean density of this fraction, $\delta\rho_{20} = N_0(a)g_0(a)\delta a$ is the mean density of the same fraction in the initial state, and $\delta\rho_2'$ is the mean density perturbation: $\delta\rho_2 = \delta\rho_{20} + \delta\rho_2'$. In this case, we have

$$\int_{\Delta a}\delta\rho_2 da = \rho_2,\ \int_{\Delta a}\delta\rho_{20}da = \rho_{20},\ \int_{\Delta a}\delta\rho_2' da = \rho_2'.$$

The linearized conservation of mass equation for vapor–gas bubbles with an unperturbed mean density $\delta\rho_{20}$ has the form

$$\frac{\partial}{\partial t}(\delta\rho_2') + \delta\rho_{20}\left(\frac{\partial v_1'}{\partial r} + \theta\frac{v_1'}{r}\right) = N_0 j'\delta a.$$

Integrating this equation over the bubble radius from $a_{\min}$ to $a_{\max}$, we obtain

$$\frac{\partial\rho_2'}{\partial t} + \rho_{20}\left(\frac{\partial v_1'}{\partial r} + \theta\frac{v_1'}{r}\right) = \int_{\Delta a} N_0(a)j' da.$$

In a similar way, other conservation of mass equations take the form

$$\frac{\partial \rho_1'}{\partial t} + \rho_{10}\left(\frac{\partial v_1'}{\partial r} + \theta \frac{v_1'}{r}\right) = -\int\limits_{\Delta a} N_0(a) j' da,$$

$$\frac{\partial \rho_V'}{\partial t} + \rho_{V0}\left(\frac{\partial v_1'}{\partial r} + \theta \frac{v_1'}{r}\right) = \int\limits_{\Delta a} N_0(a) j' da.$$

The equations describing the conservation of the number of bubbles and the conservation of momentum remain unchanged after integration. The equations describing the conservation of energy and heat transfer to the bubble surface take the following form after integration:

$$\rho_{10} c_{p1} \frac{\partial T_1'}{\partial t} = \int\limits_{\Delta a} N_0(a) q_{1\Sigma} da,$$

$$\rho_{20} c_{p2} \frac{\partial T_2'}{\partial t} = \alpha_{20} \frac{\partial p_2'}{\partial t} + n_0 q_{2\Sigma},$$

$$\int\limits_{\Delta a} N_0(a) q_{1\Sigma} da + \int\limits_{\Delta a} N_0(a) q_{2\Sigma} da = -l_0 \int\limits_{\Delta a} N_0(a) j' da.$$

To simplify the above equations, we introduce the linear averaging operator

$$\langle h \rangle = \frac{1}{\rho_{20}} \int\limits_{\Delta a} N_0(a) g_0(a) h da, \quad \rho_{20} = \int\limits_{\Delta a} N_0(a) g_0(a) da.$$

Using this operator together with the definitions of heat flows and phase interaction intensity, we represent the above equations in the form

$$\begin{gathered}
\frac{\partial \rho_1'}{\partial t} + \rho_{10}\left(\frac{\partial v_1'}{\partial r} + \theta \frac{v_1'}{r}\right) = -\rho_{20} J', \quad J' = \frac{1}{1 - k_{V0}} \\
\times \left\langle \frac{k_{V\Sigma}' - k_V'}{\tau_m} \right\rangle, \quad \frac{\partial \rho_V'}{\partial t} + \rho_{V0}\left(\frac{\partial v_1'}{\partial r} + \theta \frac{v_1'}{r}\right) = \rho_{20} J', \\
\frac{\partial \rho_2'}{\partial t} + \rho_{20}\left(\frac{\partial v_1'}{\partial r} + \theta \frac{v_1'}{r}\right) = \rho_{20} J', \quad \frac{\partial n'}{\partial t} \\
+ n_0\left(\frac{\partial v_1'}{\partial r} + \theta \frac{v_1'}{r}\right) = 0, \quad \rho_{10} \frac{\partial v_1'}{\partial t} + \frac{\partial p_1'}{\partial x} = 0, \\
\frac{\partial T_1'}{\partial t} = m \left\langle \frac{T_\Sigma' - T_1'}{\tau_{T1}} \right\rangle, \quad \frac{\partial T_2'}{\partial t} = \frac{1}{\rho_2^\circ c_{p2}} \frac{\partial p_2'}{\partial t} + \frac{T_\Sigma' - T_2'}{\tau_{T2}}, \\
c_{p1} \left\langle \frac{T_\Sigma' - T_1'}{\tau_{T1}} \right\rangle + c_{p2} \left\langle \frac{T_\Sigma' - T_2'}{\tau_{T2}} \right\rangle = -l_0 J'.
\end{gathered} \tag{1}$$

To describe the radial motion of bubbles with allowance for mass transfer, we use the expressions [26, 27]

$$\frac{\partial a'}{\partial t} = w' + \frac{m^\circ a}{3} J', \quad m^\circ = \frac{\rho_{20}^\circ}{\rho_{10}^\circ}. \tag{2}$$

According to [28], we assume that the velocity of radial motion w' consists of two components: $w' = w_R' + w_A'$. Component w_R' is described by the Rayleigh–Lamb equation, and component w_A' is the acoustic term determined from the solution to the problem of spherical unloading of a spherical bubble in an acoustic field:

$$a \frac{\partial w_R'}{\partial t} + \frac{4\nu_1}{a} w_R' = \frac{p_2' - p_1'}{\rho_{10}^\circ}, \quad w_A' = \frac{p_2' - p_1'}{\rho_{10}^\circ C_1 \alpha_{20}^{1/3}}, \tag{3}$$

where ν_1 is the kinematic viscosity of the liquid and C_1 is the sound velocity in the liquid.

As the equations of state, we use the following linearized relations [21]:

$$p_1' = C_1^2 \rho_1'^\circ, \quad \frac{p_2'}{p_0} = \frac{\rho_2'^\circ}{\rho_2^\circ} + \Delta R k_V' + \frac{T_2'}{T_0}. \tag{4}$$

The condition that the vapor is saturated at the interface has the form [21]

$$\begin{gathered}
\frac{T_\Sigma'}{T_0} = E k_{V\Sigma}' + G \frac{p_2'}{p_0}, \quad \Delta R = \frac{R_{V0} - R_{G0}}{R_{20}}, \\
E = \frac{R_{V0} R_{G0}}{R_{20}^2}, \quad G = k_{V0} \frac{R_{V0}}{R_{20}}, \quad R_{20} = k_{V0} R_{V0} + k_{G0} R_{G0},
\end{gathered} \tag{5}$$

where R_{V0} and R_{G0} are the vapor and gas constants.

Thus, we have a closed system of equations (1)–(5) describing the propagation of plane, spherical, and cylindrical sound waves in a liquid with polydisperse vapor–gas bubbles. The value of parameter $\theta = 0$ corresponds to plane waves in a Cartesian coordinate system; $\theta = 1$ corresponds to cylindrical waves in a cylindrical coordinate system; and $\theta = 2$ corresponds to spherical waves in a spherical coordinate system.

DISPERSION RELATION

We investigate the solutions to system of equations (1)–(5) in the form of propagating waves for disturbances φ', where $\varphi' = v_1', \rho_1', w', \ldots$:

$\varphi' = A_\varphi \exp[i(K_* r - \omega t)]$ for plane waves,

$\varphi' = A_\varphi H_0^{(1)}(K_* r) \exp[-i\omega t]$ for cylindrical waves,

$\varphi' = \dfrac{A_\varphi}{r} \exp[i(K_* r - \omega t)]$ for spherical waves.

Here, $K_* = K + iK_{**}$– is the complex wave number, K_{**} is the linear attenuation coefficient, ω is the frequency of disturbances, and $H_0^{(1)}(z)$ is the Hankel function. Substituting this type of solutions in the system of equations, we obtain a system of linear algebraic equations in unknown amplitudes A_φ. Eliminating the unknown amplitudes, from the condition of uniqueness of a nontrivial solution to the linear system of equations, we derive a unified dispersion relation for all the wave types:

$$\left(\frac{K_*}{\omega}\right)^2 = \frac{1}{C_f^2} + 3\alpha_{20}\rho_{10}\frac{Q(H_8 + H_3) - \Omega(1 - H_4)}{1 + Z}, \quad (6)$$

where

$$Z = \frac{H_7 H_2}{H_5} - H_4,\ Q = \frac{H_2}{H_5},\ \Omega = \frac{H_1 + H_6}{H_5},$$

$$H_1 = 3T_0 V_1\left\langle\frac{t_3}{St_2}\right\rangle + \frac{3}{E}\left\langle\frac{t_m}{St_2}\right\rangle,\ V_1 = \frac{\langle L_2\rangle}{\langle L_1\rangle},$$

$$H_2 = c_{p1}V_1\langle t_1\rangle,\ H_3 = 3mT_0\left(\left\langle\frac{t_1}{t_2}\right\rangle\left\langle\frac{t_3}{St_2}\right\rangle V_2 - \left\langle\frac{t_1}{St_2}\right\rangle\right),$$

$$V_2 = \frac{R_1}{\langle L_1\rangle},\ H_4 = m\langle t_1\rangle\left(1 - c_{p1}V_2\left\langle\frac{t_1}{t_2}\right\rangle\right),\ t_1 = \frac{1}{i\omega\tau_{T1}},$$

$$S = \frac{i\omega h\rho_{10}^{\circ}a^2}{1 + ht},\ H_5 = V_1\langle M_4 S\rangle - \frac{1}{ET_0}\left\langle\frac{M_1 t_m S}{t_2}\right\rangle,$$

$$h = \frac{4\nu_1}{a^2} - i\omega,\ t = \frac{a}{C_1(\alpha_{20})^{1/3}},$$

$$H_6 = V_1\langle M_4\rangle - \frac{1}{ET_0}\left\langle\frac{M_1 t_m}{t_2}\right\rangle,$$

$$H_7 = \langle M_3 S\rangle - mV_2\langle M_4 S\rangle\left\langle\frac{t_1}{t_2}\right\rangle,$$

$$H_8 = -\langle M_3\rangle + mV_2\langle M_4\rangle\left\langle\frac{t_1}{t_2}\right\rangle,$$

$$M_1 = \frac{3T_0}{S} - \frac{T_0}{p_0} - \frac{\alpha_{20}}{\rho_{20}c_{p2}}t_2\left(1 - \frac{1}{t_2}\right),$$

$$M_2 = \frac{GT_0}{p_0}t_3 + \frac{\alpha_{20}}{\rho_{20}}t_2,\ L_1 = \frac{l_0}{k_{G0}} + R_1\frac{t_3}{t_2},$$

$$L_2 = 1 - \frac{R_1}{ET_0}\frac{t_m}{t_2} - t_m,\ M_3 = m\frac{GT_0}{p_0}t_1 - m\frac{M_1 t_1}{t_2},$$

$$M_4 = M_2 - \frac{t_3 M_1}{t_2},\ t_m = \frac{1}{i\omega\tau_m},\ t_2 = \frac{1}{1 - i\omega\tau_{T2}},$$

$$t_3 = c_{p1}t_1 - c_{p2}t_2,\ R_1 = \left(\Delta R + \frac{1 - m^{\circ}}{k_{G0}}\right)T_0,\ C_f = \frac{C_1}{\alpha_{10}}.$$

We consider the problem for the case of sound wave propagation in an unbounded medium. Thus, the phase velocity and attenuation coefficient are independent of the wave geometry. This confirms the statement [29] that the characteristics of plane sound waves coincide with the characteristics of spherical and cylindrical waves at sufficiently long distances from the source. Since, unlike plane waves, spherical and cylindrical waves attenuate in the absence of dissipation because of their geometric divergence, the geometry of the disturbances considerably affects the evolution of pressure pulses (this will be demonstrated below).

Let us consider the specific case where $k_{V0} = 1$, $k_{G0} = 0$, i.e., the liquid contains vapor bubbles alone. In this case, we have

$$\Delta R = 1,\ G = 1,\ E = 1,\ V_1 = \frac{(m^{\circ} - 1)\langle t_m/t_2\rangle}{\langle l_0 + T_0(1 - m^{\circ})t_3/t_2\rangle},$$

$$V_2 = \frac{(1 - m^{\circ})T_0}{\langle l_0 + T_0(1 - m^{\circ})t_3/t_2\rangle}.$$

EQUILIBRIUM SOUND VELOCITY IN A VAPOR–GAS–LIQUID MIXTURE

The expression for the equilibrium sound velocity in a vapor–gas–liquid mixture is obtained from the dispersion relation by passing to the limit $\omega \to 0$:

$$C_e^2 = \frac{p_0}{\rho_{10}}\frac{\xi_4}{\xi_1 + \xi_2 - \xi_3}, \quad (7)$$

where

$$\xi_1 = k_{G0}m_1\alpha_{20}(ET_0 + GR_1),\ \xi_2 = (1 - G)\frac{ml_0\alpha_{20}}{c_{p1}},$$

$$\xi_3 = \frac{k_{G0}\alpha_{20}p_0 m}{\rho_{20}^{\circ}c_{p1}}\left(\frac{R_1}{T_0} + E\right),\ \xi_4 = \frac{ml_0}{c_{p1}} + m_1 k_{G0}ET_0,$$

$$m_1 = 1 + m\frac{c_{p2}}{c_{p1}},\ R_1 = \left(\Delta R + \frac{1 - m^{\circ}}{k_{G0}}\right)T_0,$$

$$m = \frac{\alpha_{20}}{\alpha_{10}}m^{\circ},\ m^{\circ} = \frac{\rho_{20}^{\circ}}{\rho_{10}^{\circ}}.$$

The expression for the equilibrium sound velocity for a vapor–gas–liquid mixture is determined from Eq. (7) by applying the passage to the limit, which yields $k_{V0} \to 1$:

$$C_e^2 = \frac{p_0 l_0 m\rho_{V0}^{\circ}}{(mp_0 - c_{p1}m_1T_0\rho_{V0}^{\circ})(m^{\circ} - 1)\alpha_{20}\alpha_{10}\rho_{10}^{\circ}},$$

$$m^{\circ} = \frac{\rho_{V0}^{\circ}}{\rho_{10}^{\circ}}. \quad (8)$$

If the liquid contains only gas bubbles, i.e., $k_{V0} \to 0$, the equilibrium velocity takes the form [9, 24]

$$C_e^2 = \frac{p_0}{\alpha_{20}\alpha_{10}\rho_{10}^{\circ}}. \quad (9)$$

CALCULATION RESULTS

We consider the propagation of sound waves in a mixture of water with vapor–gas bubbles for the following parameters of the mixture: $p_0 = 0.1$ MPa, $327 < T_0 < 371$ K, $\mathrm{Nu}_1 = 2$, $\mathrm{Nu}_2 = 10$, and $\mathrm{Sh}_1 = 1$. We perform the calculations using dispersion relation (6).

Figure 1 shows the influence of the polydisperse nature of bubbles with different distribution functions in Fig. 2 on the dependences of the phase velocity and

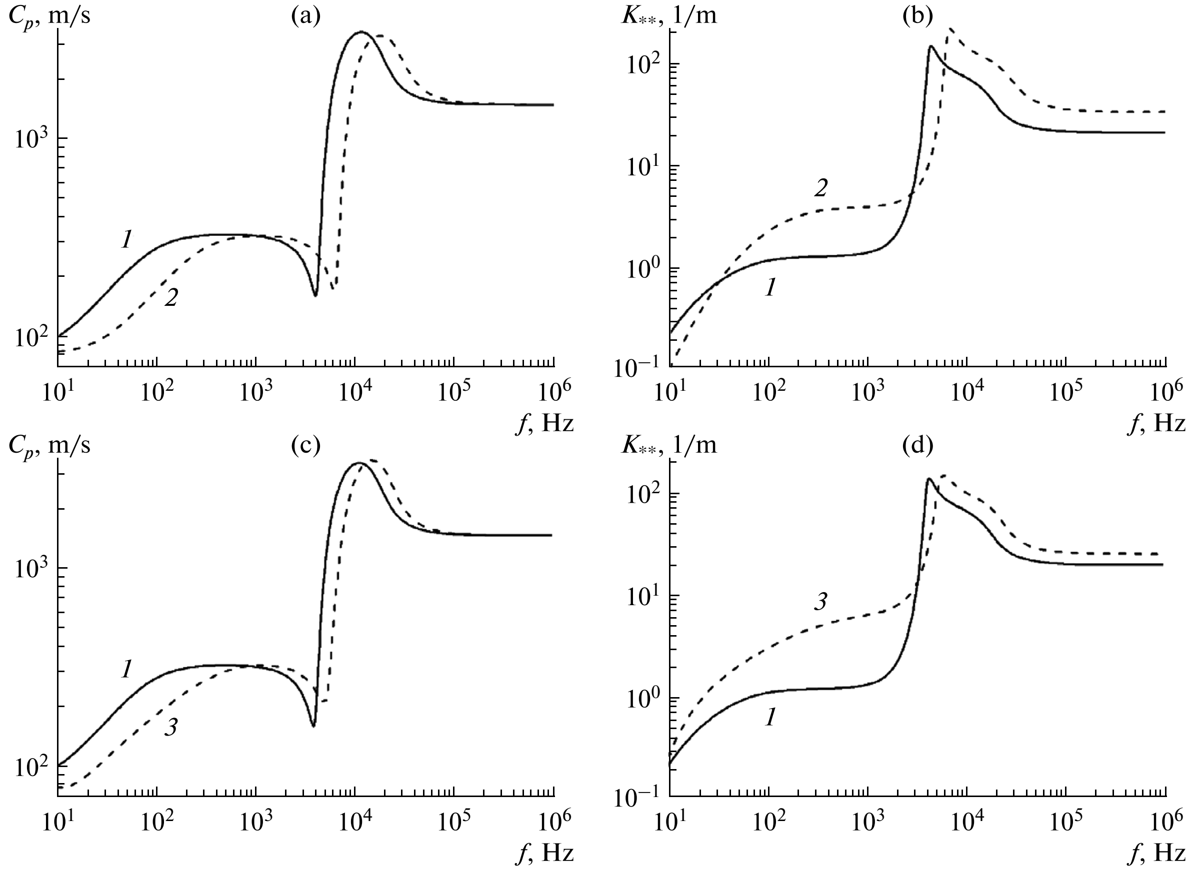

Fig. 1. (a, c) Dependences of phase velocity and (b, d) attenuation coefficient on frequency of disturbances in mixture of water with polydisperse vapor–air bubbles (*1, 2*) for different bubble size distributions and (*3*) for the case of monodisperse bubbles.

attenuation coefficient on the frequency of disturbances $f = \omega/2\pi$. The volume content of the bubbles is $\alpha_{20} = 0.001$, the initial vapor concentration in the bubbles is $k_{V0} = 0.9$, and the bubble radius a varies between 10^{-4} and 10^{-3} m. Curves *1* correspond to the Gaussian distribution function

$$N_0(a) = \frac{1}{s\sqrt{2\pi}}\exp\left[-\frac{(a-a_0)^2}{2s^2}\right], \quad a_0 = \frac{a_{\min} + a_{\max}}{2}, \quad (10)$$

curves *2* correspond to the Rayleigh distribution function

$$N_0(a) = \frac{a}{s^2}\exp\left(-\frac{a^2}{2s^2}\right). \quad (11)$$

In the calculations, the distribution parameter s is taken as 0.21×10^{-3} m. Now, it is important to note several points. First, the presence of bubbles in the liquid leads to the appearance of a phase velocity minimum and an attenuation maximum in the vicinity of the natural (resonance) frequency. For the bubble size under consideration, the natural vibration frequency is little affected by heat and mass transfer and by viscosity [1, 26]; hence, the natural frequency can be determined from the Minnaert formula $\omega_0 = \frac{1}{a_0}\sqrt{\frac{3\gamma p_0}{\overset{\circ}{\rho}_{10}}}$, where γ is the adiabatic index. Second, since the maximum of the Rayleigh function occurs for a smaller bubble size, as compared to the maximum of the Gaussian function (Fig. 2), the phase velocity minimum and the attenuation maximum are observed for the Rayleigh function at higher frequencies (Figs. 1a and 1b). Third, for monodisperse bubbles, the attenuation coefficient takes on higher values, whereas for polydisperse bubbles, the corresponding values are much smaller in a broad frequency range (Fig. 1d). Hence, according to Fig. 1, the polydisperse nature of bubbles and the form of the distribution function strongly influence the positions of the dispersion curves.

Figure 3 demonstrates the effect of the initial vapor concentration in the bubbles on the dependences of the phase velocity and the attenuation coefficient on the disturbance frequency for the aforementioned parameters of the mixture. Curves *1* correspond to the vapor concentration $k_{V0} = 0.1$ and the temperature $T_0 = 327$ K; curves *2* to $k_{V0} = 0.5$ and $T_0 = 360$ K; and curves *3* to $k_{V0} = 0.9$ and $T_0 = 371$ K. For the calcula-

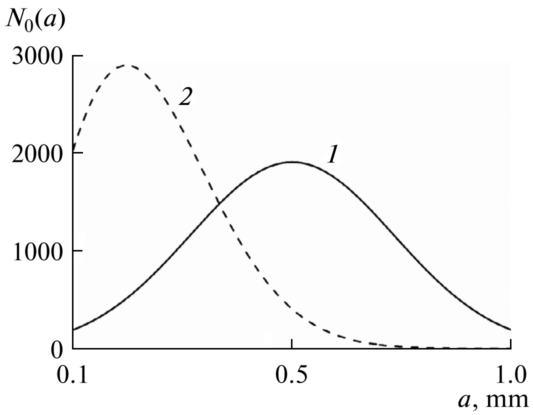

Fig. 2. Distribution functions representing different bubble size distributions.

tions, we choose the Rayleigh distribution function (11). An increase in the initial vapor concentration in the bubbles leads to a decrease in phase velocity (from 300 to 85 m/s) and an increase in the attenuation coefficient for frequencies below the bubble resonance frequency.

Figure 4 shows the effect of vapor concentration by the example of the evolution of a Gaussian-type pressure pulse for plane and cylindrical waves according to the calculations based on the fast Fourier transform, as in [30]. The calculated profiles are constructed for distances of 1.3 and 2.5 m from the pulse generation point. One can see that, as a result of the considerable effect of the initial vapor concentration in the bubbles on the dispersion and dissipation of harmonic disturbances, an increase in k_{V0} leads to a considerable decrease in the initial pulse amplitude in both plane and cylindrical cases.

COMPARISON OF THEORY AND EXPERIMENT

In [31], the results of measuring the velocity of plane sound waves in water with vapor bubbles are presented for the following parameters of the mixture: $p_0 = 0.1$ MPa and $T_0 = 373$ K. The bubble radius a varied within 10^{-5} to 10^{-4} m. The volume content was not measured with sufficient accuracy. The authors approximately estimated this quantity to be within 0.03 to 0.3%.

Figure 5 compares the dependences of the phase velocity on the disturbance frequency with the measured data. The theoretical curves correspond to three cases: (*1*) $k_{V0} = 0$ (a gas–liquid mixture), (*2*) $k_{V0} = 0.9$ (a vapor–gas–liquid mixture), and (*3*) $k_{V0} = 1$ (a vapor–liquid mixture). The calculations were performed for the bubble size distribution given by function (10) with the distribution parameter $s = 1$. The volume content was assumed to be 0.14%. In spite of the scatter of experimental data, it is possible to observe the effect of phase transitions. Namely, one can clearly see the phase velocity decrease at frequencies below the bubble resonance frequency. At a frequency of 100 Hz, for bubbles containing 90% vapor and 10% air, the sound velocity is 69 m/s, whereas for purely vapor bubbles, the sound velocity is 23 m/s. In [18, 19], it was experimentally demonstrated that in a vapor–water medium, at low frequencies (~1 Hz), the sound velocity (the so-called low-frequency effective sound velocity) can be several meters per second.

Figure 6 compares the dependences of the low-frequency effective sound velocity on the gas or vapor volume content with experimental data. Curve *1* is plotted according to Eq. (9) for an air–water mixture at a pressure of $p_0 = 0.1$ MPa; curve *2* is plotted according to Eq. (8) for a vapor–water mixture at a pressure of $p_0 = 0.2$ MPa. One can see that the low-frequency velocity in the gas–liquid mixture widely differs from

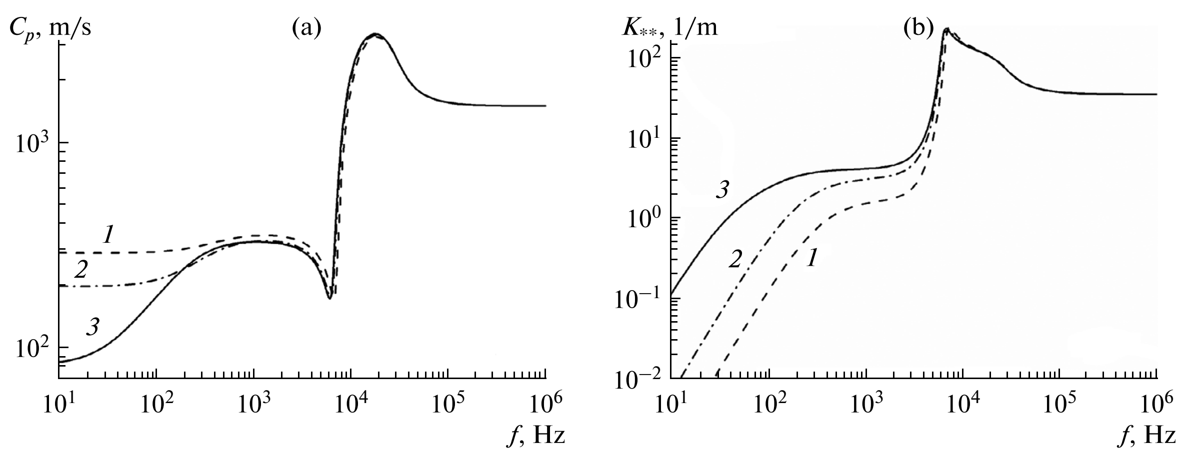

Fig. 3. Dependences of (a) phase velocity and (b) attenuation coefficient on frequency of disturbances for different values of initial vapor concentration in bubbles.

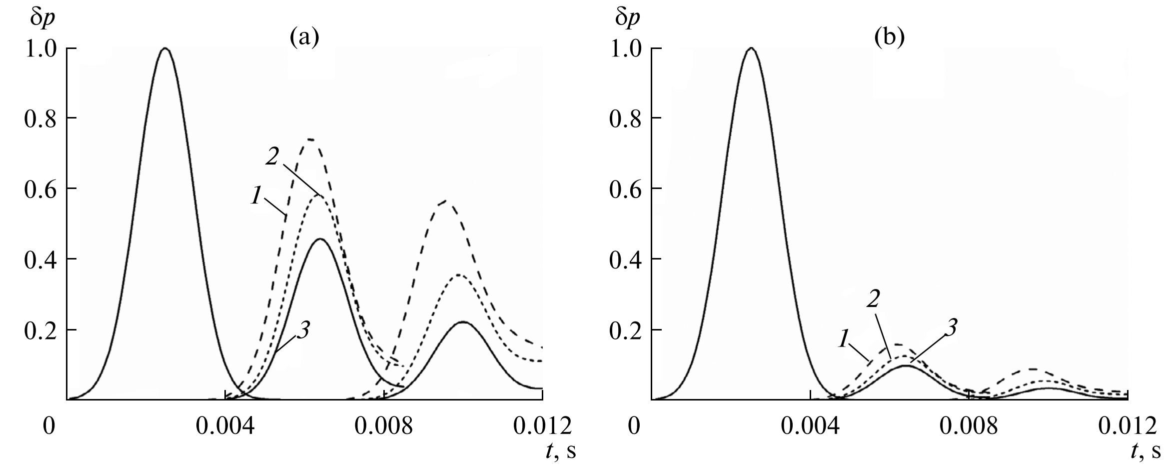

Fig. 4. Evolution of (a) plane and (b) cylindrical pressure waves in mixture of water with vapor–gas bubbles for different values of initial vapor concentration in bubbles.

the low-frequency velocity in the vapor–liquid mixture, which is confirmed by experimental data. The authors of [18] have found that, with an increase in the volume content of vapor, the velocity of low-frequency disturbances remained approximately constant, tending to the Landau sound velocity [20]. Theoretical curve *2* exhibits a monotonic increase, but on the whole, it agrees with the experimental data.

Figure 7 compares the dependences of the low-frequency effective sound velocity on the volume content of vapor with the experimental data [33]. The theoretical curve is constructed for R404A freon at a saturation temperature of 293 K. The calculations were performed with Eq. (8). In the experiment, the characteristic frequency of the input disturbance was 0.2–5 Hz. For the aforementioned mixture, with allowance for phase transformations in the region of moderate vapor contents, the sound velocity is rather low, about 5 m/s for a volume content of $\alpha_{20} = 0.4$. As the volume content of vapor increases, the velocity of the low-frequency disturbances grows; as the volume content approaches unity, it tends to the sound velocity in pure vapor. The theoretical curves agree well with experimental data for vapor contents up to 90%. At high vapor contents, the experimental values of the low-frequency sound velocity take on higher values, as compared to theoretical ones.

Thus, we obtain fair agreement of the theoretical phase velocity curves with experimental data, which testifies to the suitability of the dispersion relation derived above for describing sound wave propagation in vapor–gas–liquid mixtures.

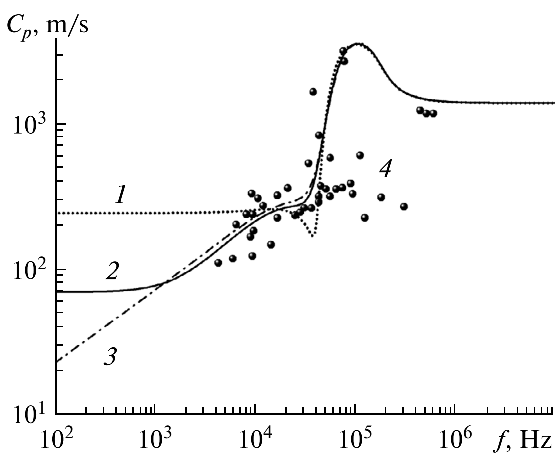

Fig. 5. Comparison of (*1–3*) calculated phase velocity values with (*4*) experimental data.

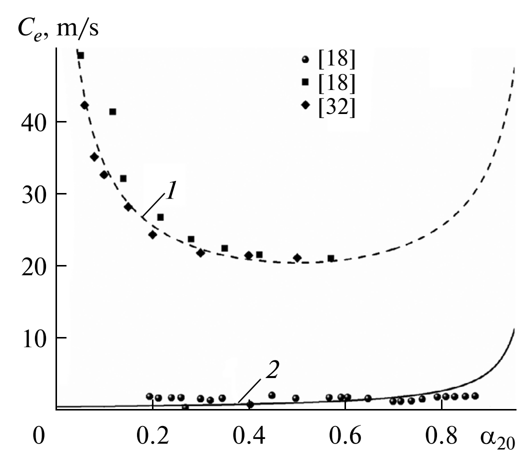

Fig. 6. Comparison of dependences of equilibrium sound velocity on gas or vapor volume content with experimental data.

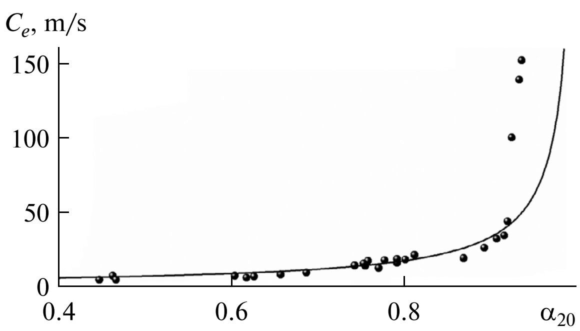

Fig. 7. Comparison of dependences of equilibrium sound velocity on vapor volume content with experimental data [33].

CONCLUSIONS

The propagation of plane, spherical, and cylindrical sound waves in a mixture of liquid with polydisperse vapor–gas bubbles is theoretically investigated with allowance for phase transitions. The dispersion relation is derived, and the equilibrium sound velocity in the vapor–gas–liquid mixture is determined. It is shown that an increase in the vapor concentration in bubbles leads to a decrease in the phase velocity and an increase in the attenuation coefficient at frequencies below the bubble resonance frequency. The effect of vapor concentration on the evolution of plane and cylindrical pressure pulses is illustrated. It is shown that the bubble distribution function considerably affects the form of the dispersion curves. The theoretical curves obtained for the phase sound velocity are found to be in fair agreement with experimental data.

ACKNOWLEDGMENTS

This work was supported by the Russian Science Foundation (project no. 15-11-20022).

REFERENCES

1. R. I. Nigmatulin, *Dynamics of Multiphase Systems* (Nauka, Moscow, 1987), Part 1.
2. V. E. Nakoryakov, B. G. Pokusaev, and I. R. Shreiber, *Wave Mechanics of Gas- and Vapor—Liquid Media* (Energoatomizdat, Moscow, 1990) [in Russian].
3. A. A. Gubaidullin, A. I. Ivandaev, R. I. Nigmatulin, and N. S. Khabeev, in *Resume of Science and Technics. Mechanics of Liquid and Gas* (VINITI, Moscow, 1982), Vol. 17, pp. 160–249.
4. A. Yu. Varaksin, High Temp. **51**, 377 (2013).
5. V. Sh. Shagapov, Prikl. Mekhan. Tekhn. Fiz. **18**, 90 (1977).
6. K. W. Commander and A. Prosperetti, J. Acoust. Soc. Am. **85**, 732 (1989).
7. V. N. Alekseev and S. A. Rybak, Acoust. Phys. **43**, 633 (1997).
8. V. N. Alekseev and S. A. Rybak, Acoust. Phys. **45**, 535 (1999).
9. D. A. Gubaidullin and Yu. V. Fedorov, J. Appl. Mat. Mech. **77**, 532 (2013).
10. P. S. Wilson, R. A. Roy, and W. M. Carey, J. Acoust. Soc. Am. **117**, 1895 (2005).
11. V. Leroy, A. Strybulevych, J. H. Page, and M. G. Scanlon, J. Acoust. Soc. Am. **123**, 1931 (2008).
12. V. Duro, D. R. Rajaona, D. Decultot, and G. Maze, IEEE J. Oceanic Eng. **36**, 114 (2011).
13. R. I. Nigmatulin, D. A. Gubaidullin, and Yu. V. Fedorov, Dokl. Phys. **58**, 261 (2013). DOI: 10.1134/S1028335813060128
14. D. A. Gubaidullin, D. D. Gubaidullina, and Yu. V. Fedorov, Fluid Dynamics, **48**, 781 (2013).
15. V. E. Nakoryakov, B. G. Pokusaev, N. A. Pribaturin, and I. R. Shreiber, Akust. Zh. **30**, 808 (1984).
16. D. S. Drumheller and A. Bedford, J. Acoust. Soc. Am. **67**, 186 (1980).
17. K. H. Ardron and R. B. Duffey, Int. J. Multiphase Flow **4**, 303 (1978).
18. B. G. Pokusaev, E. A. Tairov, and S. A. Vasil'ev, Acoust. Phys. **56**, 306 (2010).
19. B. G. Pokusaev, E. A. Tairov, A. S. Safarov, and D. A. Nekrasov, Therm. Sci. **18**, 591 (2014).
20. L. D. Landau and E. M. Lifshitch, *Fluid Mechanics. Vol. 6 of Theor. Phys. Course* (Butterworth-Heinemann, 1987, 2nd ed.; Nauka, Moscow, 1988).
21. A. Sh. Azamatov and V. Sh. Shagapov, Akust. Zh. **27**, 161 (1981).
22. D. A. Gubaidullin and A. A. Nikiforov, High Temper. **48**, 170 (2010).
23. V. A. Grigor'ev, A. A. Lun'kov, and V. G. Petnikov, Acoust. Phys. **61**, 85 (2015).
24. V. Sh. Shagapov and V. V. Sarapulova, Acoust. Phys. **61**, 37 (2015).
25. V. A. Gusev and O. V. Rudenko, Acoust. Phys. **61**, 152 (2015).
26. R. I. Nigmatulin, N. S. Khabeev, and F. B. Nagiev, Int. J. Heat Mass Transfer **24**, 1033 (1981).
27. N. S. Khabeev, Int. J. Heat Mass Transfer **50**, 4323 (2007).
28. V. Sh. Shagapov, I. K. Gimaltdinov, N. S. Khabeev, and S. S. Bailey, Shock Waves **13**, 49 (2003).
29. V. A. Krasil'nikov, *Introduction into Acoustics. A Tutorial* (MGU, Moscow, 1992) [in Russian].
30. D. A. Gubaidullin, *Dynamics of Two-Phase Vapor-Gas-Drop Media* (Kazan. Matem. Obshch., Kazan, 1998) [in Russian].
31. C. L. Feldman, S. E. Nydick, and R. P. Kokernak, Prog. Heat Mass Transfer **6**, 671 (1972).
32. H. B. Karplus, *The Velocity of Sound in Liquids Containing Gas Bubbles* Res. Develop./Report ARF-4132. Atomic Energy Comm.
33. W. Kuczynski, Int. J. of Heat Fluid Flow **40**, 135 (2013).

Translated by E. Golyamina